Efficient Transient Simulation of Embedded Subnetworks Characterized by S-Parameters in the Presence of Nonlinear Elements

Ramachandra Achar, *Student Member, IEEE,* and Michel S. Nakhla, *Fellow, IEEE*

***Abstract*— This paper presents an efficient technique for transient simulation of linear subnetworks characterized by S-parameters in the presence of nonlinear components. The proposed method is based on the recently developed model-reduction technique, complex frequency hopping. A new algorithm for computing the moments of S-parameter-based subnetworks is presented. The proposed method is suitable for simulating large number of S-parameter-based subnetworks in a general circuit environment consisting of lumped/distributed elements and nonlinear devices.**

***Index Terms*—Circuit simulation, complex frequency hopping, distributed networks, high-speed interconnects, model-order reduction, moment-matching techniques, RF circuits, scattering parameters.**

I. Introduction

RECENTLY, characterization and simulation of linear subnetworks characterized by scattering parameters within nonlinear simulation environment has become a topic of intense research. Important applications of scattering parameters include high-frequency microwave devices and high-speed interconnects. At higher frequencies, it may not always be possible to have analytical models for interconnects due to topological and inhomogeneity constraints. For example, in chip carriers, interconnections are usually nonuniform due to high-circuit density, complex geometry, and geometrical constraints at the edges of the chip. Nonuniform transmission lines are also used as filters, couplers, impedance matching blocks, equalizers, resonators, and pulse transformers. Also, the recent boom in wireless communications in combination with advances in silicon technology has made the on-chip inductors very popular in RF front-end integrated circuits (IC's). Generally, the behavior of such structures is characterized using frequency-dependent scattering parameters [1]–[8]. Such parameters can be obtained either directly from measurements or from rigorous full-wave electromagnetic simulation.

However, transient simulation of such frequency-dependent parameters in the presence of nonlinear devices is a CPU-expensive process. This can be attributed to the mixed frequency/time problem as the network contains both S-parameters which are characterized in the frequency-domain and nonlinear devices which are represented only in the time-domain.

There have been several attempts in the literature to address the above issue. These approaches can be broadly classified into two categories. In the first category, transient simulation is performed based on the traditional convolution process [3]–[5], wherein the frequency-domain measured data is first converted to time-domain using inverse Fourier transform and then convoluted with the transient responses of both the nonlinear load and the input excitation. However, such an approach suffers in a general circuit environment containing a large number of nonlinear devices due to computational inefficiency and convergence problems. Approaches in the second category are based on obtaining a reduced-order model [6]–[8] for the measured data and performing the transient analysis using recursive convolution [7], [9]. However, there are three main difficulties associated with these approaches: 1) lack of a systematic approach [6] to capture the entire frequency spectrum of interest from the given S-parameters; 2) CPU expense and stability problems associated with the convolution-based techniques; and 3) accuracy problems associated with the computation of moments.

A straightforward way to compute the moments is to perform direct numerical differentiation or through local rational approximations [8]. However, the difficulties in such approaches are obtaining an accurate local approximation, selection of the appropriate step size, and choosing an optimum bandwidth for such an approximation. Choosing a bandwidth much smaller or larger than the modulus of the nearest pole results in rapidly deteriorating derivative values. In the case of subnetworks characterized by time-domain measurements, an accurate moment-computation algorithm based on time-domain integration has been presented in [10]. *In this paper, we extend the time-domain integration scheme to include measured subnetworks characterized by frequency-dependent scattering parameters.* The main contributions/advantages of the new technique presented in this paper are summarized below.

- An algorithm based on the complex frequency hopping (CFH) [12], [13] is presented for the model-reduction of the global circuit matrix consisting of S-parameter-based subnetworks. This will reduce the size of the problem under consideration and results in two to three order CPU speed-up compared to previous techniques. Use of the CFH algorithm helps to preserve the frequency

Manuscript received March 30, 1998; revised August 28. 1998. This work was supported in part by the Natural Sciences and Engineering Research Council of Canada (NSERC), Micronet, Nortel, and Gennum Corporation.

The authors are with the Department of Electronics, Carleton University, Ottawa, Ont., Canada K1S 5B6.

Publisher Item Identifier S 0018-9480(98)09197-2.

spectrum of the S-parameters up to the highest frequency of interest.
- A new moment-generation scheme based on time-domain integration is developed for S-parameter-based subnetworks.
- A time-domain macromodel from the reduced-order description is derived and it can be easily stenciled into general-purpose simulators such as SPICE. As a SPICE subcircuit, the macromodel can be incorporated into a standard simulator and connected through its port nodes to either linear or nonlinear circuits and can be efficiently simulated to obtain unified transient responses [11]. This simulation scheme overcomes the problems associated with the traditional convolution techniques.

The rest of the paper is organized as follows. Section II presents a systematic approach to include linear lumped elements and linear measured subnetworks using modified nodal analysis technique. Section III presents the new model-reduction algorithm for S-parameter-based subnetworks. Section IV briefly describes the derivation of a time-domain macromodel from reduced-order descriptions for obtaining unified transient simulation. Sections V and VI present computational results and conclusions, respectively.

II. Formulation of Network Equations

In this section, a unified formulation scheme is presented to include S-parameter-based devices in a modified nodal analysis (MNA) [11]. In order to make the formulation suitable for model-reduction, the network under consideration is divided into nonlinear and linear subnetworks and the corresponding formulation is presented in the first part of this section. The linear subnetwork can contain lumped elements and measured subnetworks, and its formulation is given in the second part of this section.

A. General Formulation of Network Equations

Consider a general network ϕ containing an arbitrary number of nonlinear components and linear subnetworks. The linear subnetworks can contain linear lumped components and S-parameter-based devices. For simplicity, let all the linear subnetworks be grouped into a single linear subnetwork π as shown in Fig. 1. Without loss of generality, the MNA matrix for the network ϕ can be written as

$$\boldsymbol{L}_\pi \boldsymbol{i}_\pi(t) + \boldsymbol{F}\left(\boldsymbol{v}_\phi(t), \frac{d\boldsymbol{v}_\phi}{dt}\right) - \boldsymbol{b}_\phi(t) = 0, \quad t \in [0, T] \quad (1)$$

where
- $\boldsymbol{v}_\phi(t) \in \Re^{N_\phi}$ is the vector of node voltage waveforms appended by independent voltage source currents, linear inductor currents, nonlinear capacitor charges, and nonlinear inductor flux waveforms;
- $\boldsymbol{b}_\phi \in \Re^{N_\phi}$ is a vector with entries determined by the independent voltage/current sources;
- $\boldsymbol{F}(v_\phi)$ is a function describing the nonlinear elements of the circuit;
- $\boldsymbol{L}_\pi = [l_{i,j}]$ with elements $l_{i,j} \in \{0, 1\}$ where $i \in \{1, 2, \cdots, N_\phi\}$, $j \in \{1, 2, \cdots, n_\pi\}$ with a maximum of one nonzero in each row or column, is a selector matrix that maps $\boldsymbol{i}_\pi(t) \in \Re^{n_\pi}$, the vector of currents entering the linear subnetwork π, into the node space $\Re^{N_\phi}$ of the network ϕ;
- N_ϕ is the total number of variables in the MNA formulation;
- n_π is the total number ports associated with the linear subnetwork π.

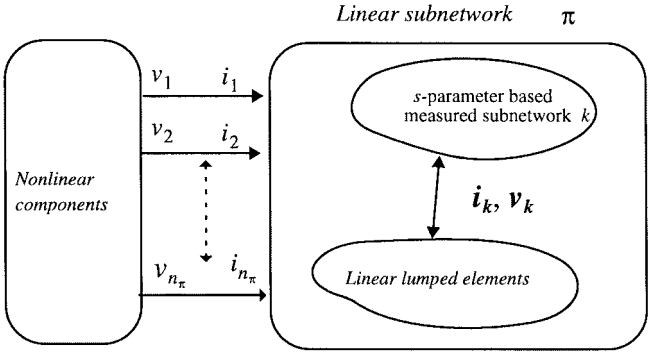

Fig. 1. Nonlinear network containing linear subnetwork.

The linear multiterminal subnetwork π can be characterized in the frequency-domain by its terminal behavior. Without loss of generality, the terminal relations for subnetwork π can be represented by frequency-domain equations in the form

$$\boldsymbol{I}_\pi(s) = \boldsymbol{Y}_\pi(s)\boldsymbol{V}_\pi(s) \quad (2)$$

where $\boldsymbol{Y}_\pi(s)$ is the frequency-domain admittance representation of the subnetwork π. $\boldsymbol{V}_\pi(s)$ and $\boldsymbol{I}_\pi(s)$ are the vector of terminal voltages/currents that connect the subnetwork π to the network ϕ.

The difficulty in solving (1) and (2) simultaneously is due to the fact that they implicitly contain a mixture of frequency- and time-domain representations. This can be efficiently addressed using the following three basic steps: a) using moment-matching techniques, $\boldsymbol{Y}_\pi(s)$ in (2) is approximated by a q-pole lower order model, b) a time-domain macromodel in the form of ordinary differential equations is derived using the lower order frequency-domain information, and c) the differential equations are solved simultaneously with (1) using standard nonlinear solvers.

B. Formulation of Linear Subnetwork π Containing S-Parameter-Based Devices

In this section, formulation of linear subnetwork π suitable for model-reduction is presented. Let the linear network π consist of lumped components and N_s linear subnetworks characterized by S-parameters. Let each S-parameter-based subnetwork k have N_k terminals (Fig. 1). The generalized circuit equations using modified nodal analysis for the entire linear subnetwork can be written as

$$\boldsymbol{C}\frac{\partial}{\partial t}\boldsymbol{v}(t) + \boldsymbol{G}\boldsymbol{v}(t) + \sum_{k=1}^{N_s} \boldsymbol{E}_k \boldsymbol{i}_k(t) - \boldsymbol{b}\partial(t) = 0, \qquad t \in [0, T] \quad (3)$$

where $\boldsymbol{Z}, \boldsymbol{G} \in \Re^{N_\pi \times N_\pi}$ are constant matrices determined by lumped linear components, $\boldsymbol{b} \in \Re^{N_\pi}$ is a constant vector with entries determined by the independent voltage/current sources, and $\boldsymbol{v}(t) \in \Re^{N_\pi}$ is the vector of node voltage waveforms appended by inductor/independent voltage source currents of linear subnetwork π, $\boldsymbol{E}_k = [e_{i,j} \in \{0,1\}]$ is a selector matrix that maps $\boldsymbol{i}_k(t) \in \Re^{N_k}$, the vector of currents entering the subnetwork k, into the node space of network π. N_π is the total number of variables in the MNA formulation, and $\delta(t)$ is the unit impulse function.

Next, the stencil of S-parameter-based subnetworks can be represented in terms of y-parameters as

$$\boldsymbol{I}_k(s) = \boldsymbol{Y}_k(s)\boldsymbol{V}_k(s) \tag{4}$$

where $\boldsymbol{I}_k(s)$ and $\boldsymbol{V}_k(s)$ are the Laplace-domain terminal current and voltage vectors and $\boldsymbol{Y}_k(s)$ is a $N_k \times N_k$ y-parameter matrix for the measured subnetwork k. The y-parameters of the linear subnetwork k are related to the S-parameters, $\boldsymbol{S}_k$, as [1]

$$\boldsymbol{Y}_k\boldsymbol{F}_k(\boldsymbol{S}_k\boldsymbol{R}_k + \boldsymbol{R}_k^*) = \boldsymbol{F}_k(\boldsymbol{I}_k - \boldsymbol{S}_k) \tag{5}$$

where

$$\boldsymbol{F}_k = \text{diag}\left[\frac{1}{2\sqrt{\text{Re}(Z_1)}} \cdots \frac{1}{2\sqrt{\text{Re}(Z_N)}}\right] \tag{6}$$

$$\boldsymbol{R}_k = \text{diag}[Z_1 \cdots Z_N]. \tag{7}$$

Here $Z_1 \cdots Z_N$ represent the reference impedances at the terminals of the subnetwork. $\boldsymbol{S}_k$, $\boldsymbol{I}_k$ are $N_k \times N_k$ S-parameter and identity matrices, respectively. "*" represents the complex Hermitian operation. Using (3) and (4), the network equation in the frequency-domain can be written as

$$\begin{bmatrix} \boldsymbol{G}+\boldsymbol{sC} & \boldsymbol{E_1} & \boldsymbol{E_2} & \cdots & \boldsymbol{E}_{\boldsymbol{N}_s} \\ \boldsymbol{Y_1}\boldsymbol{E}_1^t & -\boldsymbol{U} & 0 & 0 & 0 \\ \cdots & 0 & 0 & \cdots & 0 \\ \boldsymbol{Y}_{\boldsymbol{N}_s}\boldsymbol{E}_{\boldsymbol{N}_s}^t & 0 & 0 & 0 & -\boldsymbol{U} \end{bmatrix} \begin{bmatrix} \boldsymbol{V}(s) \\ \boldsymbol{I_1}(s) \\ \cdots \\ \boldsymbol{I}_{\boldsymbol{N}_s}(s) \end{bmatrix} = \begin{bmatrix} \boldsymbol{b} \\ 0 \\ \cdots \\ 0 \end{bmatrix} \tag{8}$$

or (8) can be concisely written as

$$\boldsymbol{H}(s)\boldsymbol{X}(s) = \tilde{\boldsymbol{b}}. \tag{9}$$

III. Development of the Proposed Model-Reduction Algorithm

In this section, a new scheme for efficient model reduction of S-parameter-based subnetworks is presented. Also, a new moment-generation algorithm for frequency-domain characterized S-parameters is described. In addition, techniques to improve the accuracy of the moments are also presented. For the benefit of the readers, this section also contains a brief review of moment-matching techniques.

A. Review of Moment-Matching Techniques

Moment-matching [12]–[16] is a technique whereby the Taylor series expansion of the network equations is used to generate, via matching, a low-order transfer function approximation. The transfer function then acts much as the entire network, both in the time- and frequency-domains. Expanding $\boldsymbol{X}(s)$ in (10) about the complex frequency point $s = \alpha$ yields

$$\boldsymbol{X}(s) = \sum_i \boldsymbol{M_n}(s-\alpha)^n\tilde{\boldsymbol{b}} \tag{10}$$

where $\boldsymbol{M_n}$ is the nth vector of coefficients (moments) of the Taylor expansion. A recursive equation for the evaluation of the moments can be obtained in the form

$$[\boldsymbol{H}(\alpha)]\boldsymbol{M_n} = -\sum_{r=1}^{n} \frac{\frac{\partial^r}{\partial s^r}\boldsymbol{H}(s)\Big|_{s=\alpha}\boldsymbol{M_{n-r}}}{r!}\tilde{\boldsymbol{b}} \tag{11}$$

with

$$[\boldsymbol{H}(\alpha)]\boldsymbol{M_0} = \tilde{\boldsymbol{b}}. \tag{12}$$

The transfer function of the system is then found by matching a Padé approximation to the moments of the system in (10). CFH [12] extends the process to multiple expansion points in the frequency range of interest. An efficient search algorithm for the selection and minimization of the expansion points as well as a method for collection of information from all the expansion points into a unified network transfer function is described in [12] and [13].

To evaluate the moments $\boldsymbol{M_n}$ using (11), the derivatives of $\boldsymbol{H}(s)$ [denoted by $\boldsymbol{H}^{(r)}$] are needed. They can be obtained using (9) as

$$[\boldsymbol{H}]^{(1)} = \begin{bmatrix} \boldsymbol{C} & 0 & 0 & \cdots & 0 \\ \boldsymbol{Y}_{\boldsymbol{1}}^{(1)}\boldsymbol{E}_{\boldsymbol{1}}^{\boldsymbol{t}} & 0 & 0 & 0 & 0 \\ \cdots & 0 & 0 & \cdots & 0 \\ \boldsymbol{Y}_{\boldsymbol{N}_s}^{(1)}\boldsymbol{E}_{\boldsymbol{N}_s}^{\boldsymbol{t}} & 0 & 0 & 0 & 0 \end{bmatrix}$$

$$[\boldsymbol{H}]^{(r)} = \begin{bmatrix} 0 & 0 & 0 & \cdots & 0 \\ \boldsymbol{Y}_{\boldsymbol{1}}^{(r)}\boldsymbol{E}_{\boldsymbol{1}}^{\boldsymbol{t}} & 0 & 0 & 0 & 0 \\ \cdots & 0 & 0 & \cdots & 0 \\ \boldsymbol{Y}_{\boldsymbol{N}_s}^{(r)}\boldsymbol{E}_{\boldsymbol{N}_s}^{\boldsymbol{t}} & 0 & 0 & 0 & 0 \end{bmatrix}, \qquad r \geq 2. \tag{13}$$

In order to perform model reduction using CFH, the individual derivatives represented by $\boldsymbol{Y}_k^{(r)}(s)$ in (13) are needed. In the next section a new algorithm for the computation of the moments is given.

B. New Moment-Generation Algorithm for S-Parameter Based Subnetworks

Consider the measured subnetwork k. The derivatives of the y-parameter matrix represented by $\boldsymbol{Y}^{(r)}(s)$ [dropping the subscript k for simplicity in (13)] can be obtained recursively using (5) as follows:

$$\boldsymbol{Y}^{(n)}\boldsymbol{P} = -\sum_{r=1}^{n}\binom{n}{r}\boldsymbol{Y}^{(n-r)}\boldsymbol{P}^{(r)} + \sum_{r=1}^{n}\binom{n}{r}\boldsymbol{F}^{(n-r)}(\boldsymbol{I} - \boldsymbol{S})^{(r)} + \boldsymbol{F}^{(n)}(\boldsymbol{I} - \boldsymbol{S}) \tag{14}$$

where

$$\boldsymbol{P} = \boldsymbol{FQ} \tag{15}$$

with

$$\boldsymbol{Q} = \boldsymbol{T} + \boldsymbol{R}^* \tag{16}$$

$$\boldsymbol{T} = \boldsymbol{SR}. \tag{17}$$

Next, derivatives of $\boldsymbol{P}$ as needed by (14), and subsequently the derivatives of $\boldsymbol{Q}$ and $\boldsymbol{T}$, can be recursively computed using (15), (16), and (17) as

$$\boldsymbol{P}^{(n)} = \sum_{r=1}^{n} \binom{n}{r} \boldsymbol{F}^{(n-r)} \boldsymbol{Q}^{(r)} + \boldsymbol{F}^{(n)} \boldsymbol{Q} \tag{18}$$

$$\boldsymbol{Q}^{(r)} = \boldsymbol{T}^{(r)} + \boldsymbol{R}^{*(r)} \tag{19}$$

$$\boldsymbol{T}^{(n)} = \sum_{r=1}^{n} \binom{n}{r} \boldsymbol{S}^{(n-r)} \boldsymbol{R}^{(r)} + \boldsymbol{S}^{(n)} \boldsymbol{R}. \tag{20}$$

However, to proceed further, (14) and (20) leave us with the task of computing the moments of s-parameters, which do not have a closed-form solution. However, to proceed further, (14) and (20) leaves us with the task of computing the moments of S-parameters, which do not have a closed-form solution, and have to be computed numerically.

In order to obtain accurate moments for frequency-domain characterized S-parameter measurements, a scheme based on time-domain integration is developed. In the proposed algorithm, given S-parameters are first converted to the time-domain using inverse fast Fourier transform. Next, the derivatives of S-parameters are obtained by performing integration in the time-domain. For the purpose of illustration, consider any individual S-parameter $\boldsymbol{s}_{i,j}(t)$ in the time-domain. Using integration in time-domain, $\boldsymbol{S}_{i,j}$ and its successive derivatives in frequency-domain can be computed as

$$\frac{d^r}{ds^r} \boldsymbol{S}_{ij}(s) = (-1)^r \int_0^{\infty} t^r \boldsymbol{s}_{ij}(t) e^{-st}\, dt. \tag{21}$$

The required derivatives at a specific frequency $s = \alpha$ (hop) during complex frequency hopping can be computed using (21).

C. Implementation and Accuracy Improvements

The calculation of inverse Fourier transform is one of the critical parts involved in the proposed algorithm for the computation of moments. Sometimes $\boldsymbol{S}_{i,j}(s)$ behaves like a periodic function as frequency approaches infinity. In such cases, obtaining the inverse Fourier transform would be difficult due to ringing and aliasing errors. In order to overcome this problem, one can use a band limiting window [4], [17]–[19] before transforming the scattering parameters to the time-domain. For this purpose, several low-pass filter windowing functions such as Hanning/Hamming window, Butterworth filter, frequency spectrum of a trapezoidal pulse, etc., can be used. However, it is to be noted that although these windowing functions improve the accuracy of the inverse Fourier transform, they alter the time-domain data, which in turn can lead to a different set of moments. In order to overcome this problem, a new scheme is developed to retrieve the original measured subnetwork moments from the band-limited inverse Fourier transform.

Consider a specific S-parameter, $\boldsymbol{S}(s)$ (subscripts i, j dropped for simplicity), which requires band limiting. In the proposed algorithm, $\boldsymbol{S}(s)$ is multiplied by the frequency spectrum of a window function $\boldsymbol{W}(s)$ of interest, and let the combined frequency response be denoted by $\Psi(s)$ as

$$\Psi(s) = \boldsymbol{S}(s)\boldsymbol{W}(s). \tag{22}$$

Let the corresponding inverse Fourier transform be denoted by $\varphi(t)$. Time-domain integration of $\varphi(t)$ will yield the combined moments $(\psi^{(r)}(s))$. Next, the required original subnetwork moments $(\boldsymbol{S}^{(r)}(s))$ are retrieved from $(\psi^{(r)}(s))$ as follows. Using (22) we can derive a recursive relationship as

$$\psi^{(n)} = \sum_{r=1}^{n} \binom{n}{r} \boldsymbol{S}^{(n-r)} \boldsymbol{W}^{(r)} + \boldsymbol{S}^{(n)} \boldsymbol{W}^{(0)}. \tag{23}$$

However, use of (23) to retrieve the original system moments $\boldsymbol{S}^{(r)}(s)$ needs the derivatives of the windowing function. The derivatives of these window functions $(\boldsymbol{W}^{(r)}(s))$ can be analytically computed. In our work, we used the Hanning function as the band-limiting window function. Closed-loop expressions for the derivatives of Hanning function were developed and the final relations are given as

$$W^{(0)} = \frac{\tau}{2}\left(\frac{\sin(\alpha s)}{\alpha s}\right)\left(\frac{1}{1+\beta s^2}\right)$$
$$\alpha = \frac{-j\tau}{2}$$
$$\beta = \left(\frac{\tau}{2\pi}\right)^2 \tag{24}$$

$$W^{(1)} = \frac{\tau}{2\alpha}\left(\left(\frac{-\sin(\alpha s)\times(1+3\beta s^2)}{(s+\beta s^3)^2}\right) + \left(\frac{\alpha\cos(\alpha s)}{(s+\beta s^3)}\right)\right) \tag{25}$$

$$W^{(2)} = \frac{\tau}{2\alpha}\left(\left(\frac{2\sin(\alpha s)\times(1+3\beta s^2)^2}{(s+\beta s^3)^3}\right) - \left(\frac{(6\beta s)\times\sin(\alpha s)}{(s+\beta s^3)^2}\right) - \left(\frac{-2\alpha\cos(\alpha s)\times(1+3\beta s^2)}{(s+\beta s^3)^2}\right) - \left(\frac{\alpha^2\sin(\alpha s)}{(s+\beta s^3)}\right)\right) \tag{26}$$

$$W^{(n)} = \frac{1}{(s+\beta s^3)}\left(\frac{\tau}{2}(-1)^k\alpha^{r-1}\binom{p\sin(\alpha s)}{q\cos(\alpha s)} - n(1+3\beta s^2)W^{n-1} - 6\beta s(n^2-n)W^{(n-2)} - \beta(n^3-3n^2-2n)W^{(n-3)}\right)$$
$$n \geq 3; \qquad k = 0 \text{ if } \frac{n}{4} = [0,\,1], \text{ else } k = 1$$
$$p = 1, \text{ if } n \text{ is even; else } p = 0$$
$$q = 1, \text{ if } n \text{ is odd; else } q = 0. \tag{27}$$

Similarly, analytical derivatives for other window functions can be derived. Since the window function moments are available in the closed-loop form, the process of retrieving system moments $\boldsymbol{S}^{(r)}(s)$ using (23) will not suffer from numerical errors. On the contrary, use of the window functions improves the IFFT, thus giving accurate $\psi^{(r)}(s)$, which in turn leads to accurate system moments.

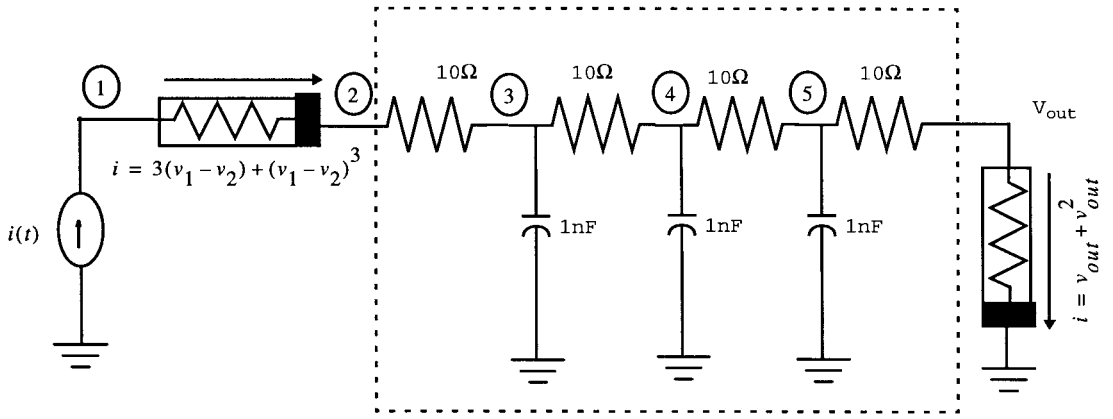

Fig. 2. Circuit for Example 1.

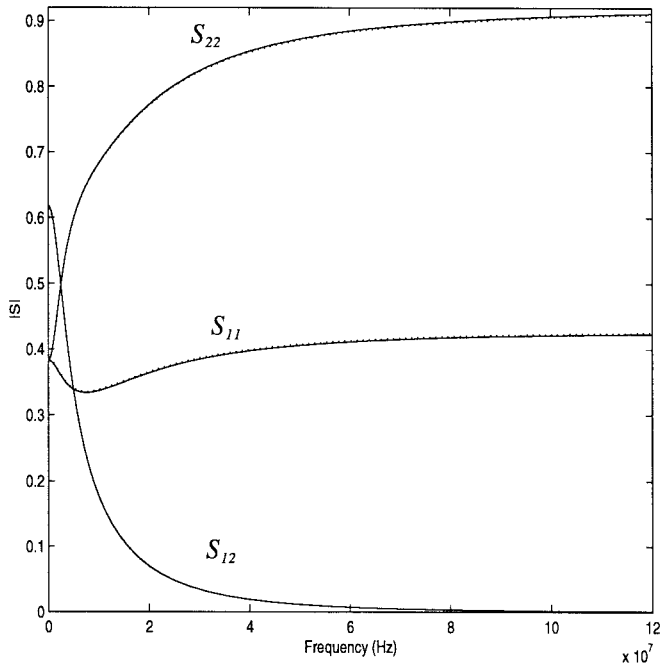

Fig. 3. S-parameters for Example 1.

Next, using the model-reduction scheme proposed in this paper, a q-pole reduced-order model is derived for the admittance matrix $\boldsymbol{Y}_\pi(s)$ in (2) as

$$\boldsymbol{Y}_\pi(s) = \begin{bmatrix} Y_{11} & Y_{12} & \cdots & Y_{1n_\pi} \\ \cdots & \cdots & \cdots & \cdots \\ Y_{n_\pi 1} & Y_{n_\pi 2} & \cdots & Y_{n_\pi n_\pi} \end{bmatrix}$$

$$Y_{jk}(s) = d^{j,k} + \sum_{i=1}^{q^{j,k}} \frac{r_i^{j,k}}{s - p_i^{j,k}}, \qquad 1 \le (j,k) \le n_\pi \quad (28)$$

where $p_i^{j,k}$ is the ith dominant pole at a port k due to an input excitation at port j and the corresponding residue is $r_i^{j,k}$. $d^{j,k}$ is the direct coupling constant. $q^{j,k}$ is the number of dominant poles used for approximating Y_{jk}. The reduced-order information in terms of poles and residues (28) is helpful in obtaining a macromodel for the linear subnetwork π and is given in the next section.

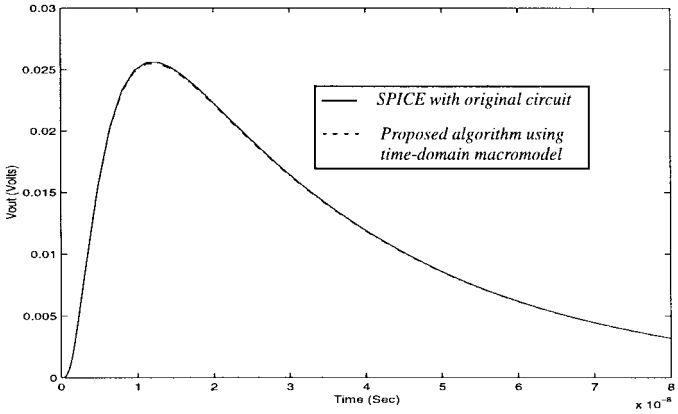

Fig. 4. Time-response for Example 1.

IV. Global Simulation Through Time-Domain Macromodels

Given a matrix-transfer function described by (28), a time-domain realization in the form of state-space equations can be obtained as [20], [21]

$$\begin{aligned} \frac{d}{dt}[\boldsymbol{z}_\pi(t)] - [\boldsymbol{A}_\pi][\boldsymbol{z}_\pi(t)] - [\boldsymbol{B}_\pi][\boldsymbol{i}_\pi(t)] &= \boldsymbol{0} \\ [\boldsymbol{v}_\pi(t)] - [\boldsymbol{C}_\pi][\boldsymbol{z}_\pi(t)] + [\boldsymbol{D}_\pi][\boldsymbol{i}_\pi(t)] &= \boldsymbol{0} \end{aligned} \quad (29)$$

where $\boldsymbol{i}_\pi$ and $\boldsymbol{v}_\pi$ are the vector of terminal currents and voltages of the linear subnetwork π. The differential equations represented by the macromodel (29) can now be combined with (1) using the relation $\boldsymbol{v}_\pi = (\boldsymbol{L}_\pi)^t \boldsymbol{v}_\phi$ as shown below

$$\begin{aligned} \frac{d}{dt}\boldsymbol{z}_\pi(t) - \boldsymbol{A}_\pi \boldsymbol{z}_\pi(t) - \boldsymbol{B}_\pi \boldsymbol{i}_\pi(t) &= 0 \\ (\boldsymbol{L}_\pi)^t \boldsymbol{v}_\phi(t) - \boldsymbol{C}_\pi \boldsymbol{z}_\pi(t) - \boldsymbol{D}_\pi \boldsymbol{i}_\pi(t) &= 0 \\ \boldsymbol{L}_\pi \boldsymbol{i}_\pi(t) + \boldsymbol{F}(\boldsymbol{v}_\phi(t)) - \boldsymbol{b}_\phi(t) &= 0. \end{aligned} \quad (30)$$

Using standard nonlinear solvers or any of the general-purpose circuit simulators, the unified set of differential equations represented by (30) can be solved to yield transient solutions for the entire nonlinear circuit consisting of measured and lumped linear components.

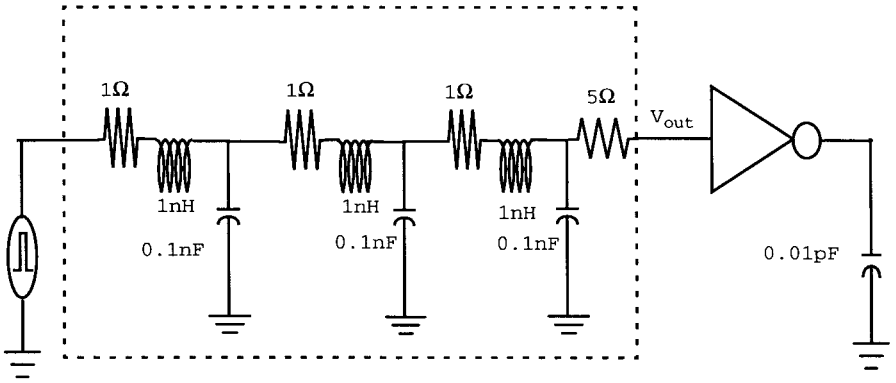

Fig. 5. Circuit for Example 2.

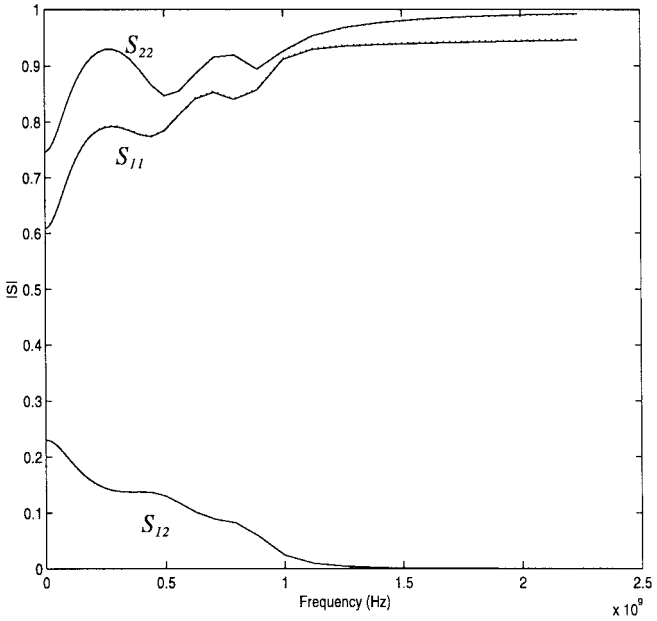

Fig. 6. S-parameters for Example 2.

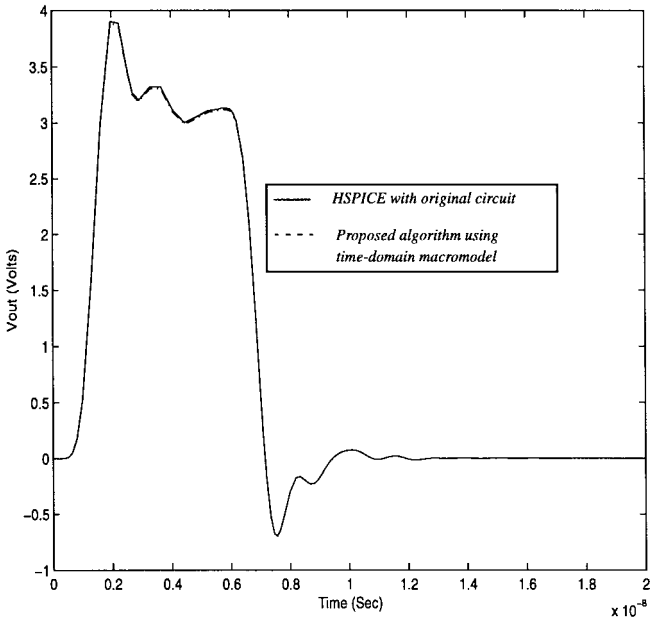

Fig. 7. Time-response for Example 2.

A. Summary of Computational Steps

A brief summary of the computational steps involved in simulating nonlinear networks comprising measured/linear lumped components using the proposed model-reduction algorithm is given below.

- *Step 1:* Formulate the global circuit MNA and obtain (1) and (2).
- *Step 2:* Consider the linear subnetwork π. Choose appropriate window functions $W(s)$ as necessary and obtain $\psi(s)$ (22) for all the S-parameters. Next, using IFFT, obtain the corresponding $\varphi(t)$.
- *Step 3:* Determine the expansion points and the number of moments using the CFH algorithm.
- *Step 4:* Compute the derivatives $\boldsymbol{W}^{(r)}(s)$, $\psi^{(r)}(s)$, and $\boldsymbol{S}^{(r)}(s)$ using (24)–(27), (21), and (23).
- *Step 5:* Compute the derivatives of y-parameters of the measured subnetwork using (14)–(20).
- *Step 6:* Repeat Steps 4 and 5 for all the measured subnetworks in linear subnetwork π.
- *Step 7:* Compute $\hat{\boldsymbol{H}}^{(r)}$ using (13).
- *Step 8:* Evaluate system moments $\boldsymbol{M_n}$ using (10)–(12) and obtain a Padé approximation.
- *Step 9:* Compute a q-pole reduced-order frequency-domain description for the admittance matrix $\boldsymbol{Y}_\pi$ of linear subnetwork π as given by (28).
- *Step 10:* Obtain a time-domain macromodel in terms of state-space equations as indicated by (29).
- *Step 11:* Solve unified set of differential equations given by (30) using SPICE or nonlinear solvers to obtain unified transient solution.

V. Computational Results

In this section, three examples are presented to demonstrate the validity and the accuracy of the proposed technique. In order to verify the accuracy of the proposed method with the existing general-purpose simulators such as SPICE, linear test circuits with known component values are chosen. Next, using SPICE, S-parameters for these networks were generated. Using these S-parameters and the proposed algorithm, equivalent time-domain macromodels were generated. Unified transient

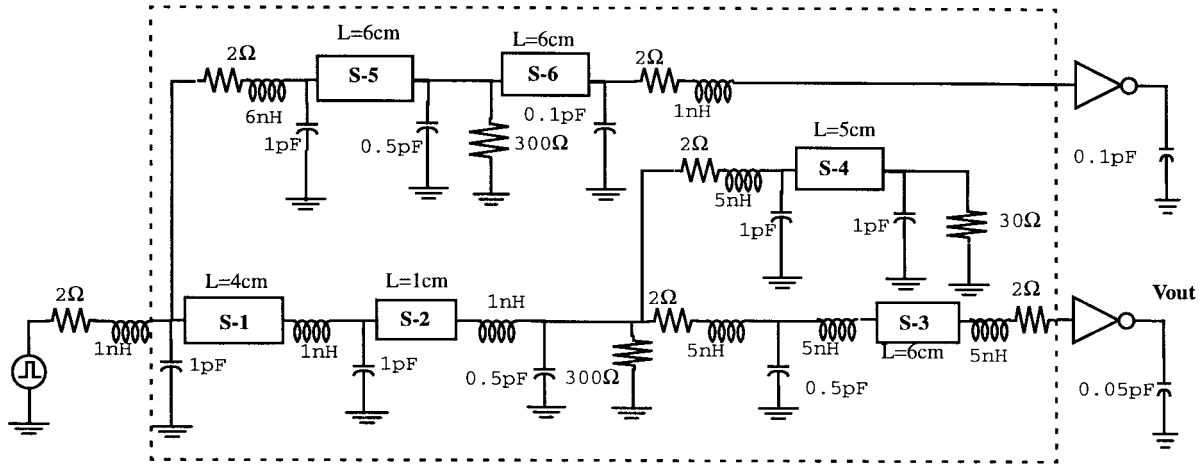

Fig. 8. Circuit for Example 3.

simulations obtained using these macromodels in the presence of nonlinear elements are compared with the simulations of the original network using SPICE. Examples 1 and 2 correspond to the RC and RLC networks, and interconnect structures are analyzed in Example 3.

Example 1: This example represents a relatively simple circuit (Fig. 2). Fig. 3 shows the S-parameters of this network obtained using HSPICE for a reference impedance of 25 Ω. The S-parameters S_{11} and S_{22} were band-limited using Hanning window function. Next, performing IFFT and subsequently an integration in the time-domain, moments of the band-limited response are obtained. Then using (23), original network moments are obtained, from which the time-domain macromodel (29) is derived. A unified transient simulation is performed using the macromodel and nonlinear terminations. These results are compared against the original network response using SPICE in Fig. 4, and they are indistinguishable.

Example 2: In this example, a simulation of S-parameters of a two-port RLC network is presented (Fig. 5). Fig. 6 shows the S-parameters of the network obtained using HSPICE for a reference impedance of 30 Ω. The S-parameters S_{11} and S_{22} were band-limited using Hanning window function. Next, using the proposed algorithm a time-domain macromodel (29) is derived. Then, a unified transient simulation is performed using the macromodel and the nonlinear terminations. Network is excited by a pulse having a rise/fall time of 0.5 ns and a pulse width of 5 ns. These results are compared against the original network response using HSPICE in Fig. 7, and they match accurately.

Example 3: The network for this example contained six transmission lines which are characterized by S-parameters. For the purpose of illustration, the S-parameters of the subnetwork #1 (represented by block S-1 in Fig. 8) are given in Fig. 9. The proposed algorithm is used to obtain a reduced-order model for the entire linear network (the network enclosed inside the dotted lines). Next, a macromodel in terms of state-space variables is derived from the reduced-order model, and a transient simulation is performed by combining the macromodel with the nonlinear elements using SPICE. Network is excited by a pulse having rise/fall time of 0.5 ns and pulse width of 5 ns. Accuracy of the results from the proposed algorithm is compared with the transient simulation of the original network using SPICE, in which each subnetwork is replaced by its quasi-TEM analytical models. Responses from both methods are given in Fig. 10 and they match accurately.

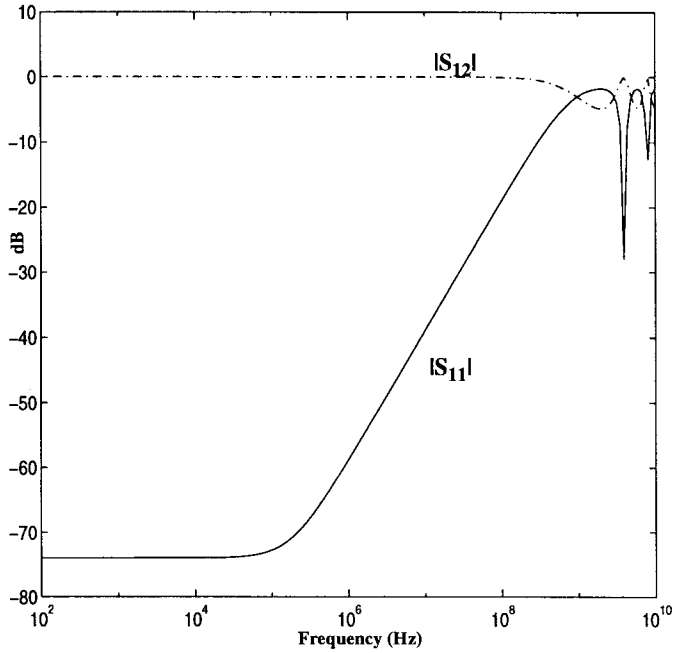

Fig. 9. S-parameters for Example 3.

VI. Conclusions

A new model-reduction scheme is developed in this paper to include measured subnetworks characterized by S-parameters in general-purpose circuit simulators such as SPICE. Also, an algorithm is presented for accurately computing the moments of the frequency-domain characterized measured S-parameters. The new technique is suitable for efficiently simulating a large number of measured subnetworks in a general circuit environment consisting of linear lumped/distributed and nonlinear components.

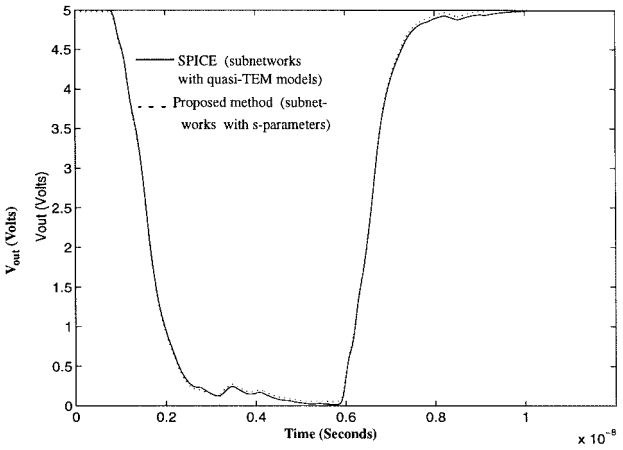

Fig. 10. Time-response for Example 3.

ACKNOWLEDGMENT

The authors wish to thank E. Ahmed of Carleton University for the help provided during the implementation of the proposed algorithm.

REFERENCES

[1] J. A. Dobrowolski, *Introduction to Computer Methods for Microwave Circuit Analysis and Design.* Norwood, MA: Artech House, 1991.
[2] W. W. M. Dai, "Special issue on simulation, modeling, and electrical design of high-speed and high-density interconnects," *IEEE Trans. Circuits Syst.,* vol. 39, no. 11, pp. 857–982, Nov. 1992.
[3] A. R. Djordjevic, T. K. Sarkar, and R. F. Harrington, "Analysis of time-domain response of lossy multiconductor transmission lines," *IEEE Trans. Microwave Theory Tech.,* vol. 34, pp. 660–665, June 1986.
[4] J. E. Schutt-Aine and R. Mittra, "Scattering parameter transient analysis of transmission lines loaded with nonlinear termination," *IEEE Trans. Microwave Theory Tech.,* vol. 36, pp. 529–536, Mar. 1988.
[5] D. Winklestein, M. B. Steer, and R. Pomeerleau, "Simulation of arbitrary transmission line networks with nonlinear terminations," *IEEE Trans. Circuits Syst.,* vol. 38, pp. 418–422, Apr. 1991.
[6] J. N. Brittingham, E. K. Miller, and J. L. Williows, "Pole extraction from real frequency information," *Proc. IEEE,* vol. 68, pp. 263–273, 1980.
[7] L. M. Silveria, I. M. Elfadel, J. K. White, M. Chilukuri, and K. S. Kundert, "An efficient approach to transmission line simulation using measured or tabulated S-parameter data," in *Proc. ACM/IEEE DAC.,* June 1994, pp. 634–639.
[8] M. Celik, A. C. Cangellaris, and A. Deutsch, "A new moment generation technique for interconnects characterized by measured or calculated S-parameters," in *IEEE Int. Microwave Symp. Dig.,* June 1996, pp. 196–201.
[9] S. Lin and E. Kuh, "Transient simulation of lossy interconnects based on the recursive convolution formulation," *IEEE Trans. Circuits Syst.,* vol. 39, pp. 869–878, Nov. 1992.
[10] G. Zheng, Q. J. Zhang, M. S. Nakhla, and R. Achar, "An efficient approach for moment-matching simulation of linear subnetworks with measured or tabulated data," in *Proc. IEEE ICCAD,* Nov. 1996, pp. 20–23.
[11] C. H. Ho, A. E. Ruehli, and P. A. Brennan, "The modified nodal approach to network analysis," *IEEE Trans. Circuits Syst.,* vol. CAS-22, pp. 504–509, June 1975.
[12] E. Chiprout and M. Nakhla, *Asymptotic Waveform Evaluation and Moment Matching for Interconnect Analysis.* Boston, MA: Kluwer, 1993.
[13] R. Sanaie, E. Chiprout, M. Nakhla, and Q. J. Zhang, "A fast method for frequency and time domain simulation of high-speed VLSI interconnects," *IEEE Trans. Microwave Theory Tech.,* vol. 42, pp. 2562–2571, Dec. 1994.
[14] D. H. Xie and M. Nakhla, "Delay and crosstalk simulation of high-speed VLSI interconnects with nonlinear terminations," *IEEE Trans. Computer-Aided Design,* vol. 12, pp. 1798–1811, Nov. 1993.
[15] L. T. Pillage and R. A. Rohrer, "Asymptotic waveform evaluation for timing analysis," *IEEE Trans. Computer-Aided Design,* vol. 9, pp. 352–366, Apr. 1990.
[16] P. Feldmann and R. W. Freund, "Efficient linear circuit analysis by Padé via Lanczos process," *IEEE Trans. Computer-Aided Design,* vol. 14, pp. 639–649, May 1995.
[17] T. Dhaene, L. Martens, and D. Zutter, "Transient simulation of arbitrary nonuniform interconnection structures characterized by scattering parameters," *IEEE Trans. Circuits Syst.,* vol. 39, pp. 928–937, Nov. 1992.
[18] W. D. Stanley, G. R. Dougherty, and R. Dougherty, *Digital Signal Processing.* Reston, VA: Reston Publishing, 1984.
[19] J. S. Walker, *Fast Fourier Transforms.* Boca Raton, FL: CRC Press, 1991.
[20] T. Kailath, *Linear Systems.* Englewood Cliffs, NJ: Prentice-Hall, 1980.
[21] C. T. Chen, *Linear System Theory and Design.* New York: Holt, Rinehart, and Winston, 1984.

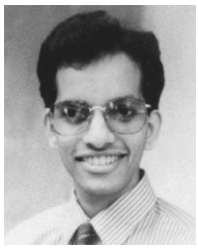

Ramachandra Achar (S'95) received the B.Eng. degree in electronics engineering from Bangalore University, India, in 1990, the M.Eng. degree in micro-electronics from Birla Institute of Technology and Science, Pilani, India, in 1992, and the Ph.D. degree from Carleton University, Ottawa, Ont., Canada, in 1998.

He is currently working as a Research Engineering in the Department of Electronics, Carleton University. He spent the summer of 1995 working on the macromodel development for linear circuits at T. J. Watson Research Center, IBM, New York. He was a Graduate Trainee at Central Electronics Engineering Research Institute, Pilani, India, during 1992. He was also previously employed at Larsen and Toubro Engineers Ltd., Mysore, India, as an R&D Engineer at their ASIC design center and at Indian Institute of Science, Bangalore, as a Research Assistant. His research interests include computer-aided design of high-speed systems and numerical algorithms.

Mr. Achar is the winner of Canadian Microelectronics Corporation Award (1996), Strategic Microelectronics Corporation Award (1997), and Micronet (a Canadian network of centers of excellence on Microelectronics) Award (1998).

Michel S. Nakhla (S'73–M'75–SM'88–F'98), for photograph and biography, see this issue, p. 2257.